Applied Energy 125 (2014) 1–9

Contents lists available at ScienceDirect

Applied Energy

journal homepage: www.elsevier.com/locate/apenergy

Velocity and turbulence effects on high intensity distributed combustion

Ahmed E.E. Khalil, Ashwani K. Gupta *

Department of Mechanical Engineering, University of Maryland, College Park, MD 20742, USA

HIGHLIGHTS

- Examined flowfield for distributed combustion for gas turbines applications.
- Role of injection velocity on flowfield and pollutants emission was examined.
- Higher air injection velocity demonstrated higher reactive gasses recirculation.
- Enhanced turbulence played critical role in mixing for non-premixed combustion mode.
- Increased injection velocity reduced NO_x emission by 20–48% under various condition.

ARTICLE INFO

Article history:
Received 27 August 2013
Received in revised form 3 November 2013
Accepted 22 November 2013
Available online 9 April 2014

Keywords:
Colorless distributed combustion (CDC)
Ultra-low NO_x and CO emission
High intensity combustion
Entrainment with air injection
Flowfield and turbulence

ABSTRACT

High intensity distributed combustion assists to provide substantial performance improvement for gas turbine applications for our quest to simultaneously seek improved pattern factor, ultra-low emission of NO_x and CO, low noise, enhanced stability, fuel flexibility and higher efficiency. In such combustion method, controlled mixing between the injected air, fuel and hot reactive gases from within the combustor prior to mixture ignition must occur to achieve distributed reactions in the entire combustion chamber. Near zero emission of NO and CO has been achieved using methane as the fuel under distributed combustion conditions at high heat (energy) release intensity of 22–36 MW/m^3 atm. The conditions to form distributed reaction in the combustor are further investigated through variation of air injection velocity with the output parameters focused on pollutants emission and combustor performance. The isothermal flowfield is examined using particle image velocimetry (PIV) to determine key features associated with the flowfield and its effects on pollutants emission and stability. The results showed higher entrainment and turbulence at increased injection velocity. Increase in injection velocity decreased NO emissions by some 20–48% with minimal impact on CO emission under premixed fuel–air condition. Less than 4 ppm of NO was achieved at an injection velocity of 46 m/s at an equivalence ratio of 0.7 and heat (energy) release intensity of 31.5 MW/m^3 atm using normal temperature air. High injection velocity at the same operating condition decreased NO emission by some 20% to 3.2 ppm. Higher injection velocity under preheated inlet air condition further decreased NO to 2 ppm (48% reduction) at an equivalence ratio of 0.5. The results under non-premixed combustion conditions showed similar behavior. The reduction of NO with single injection parameter is attributed to improved distributed reaction condition from direct entrainment and rapid mixing of reactive species present in the combustion zone under high intensity combustion conditions.

© 2014 Elsevier Ltd. All rights reserved.

1. Introduction

Combustion turbines continue to remain amongst the prime source of electric energy and combined heat and power generation due to higher efficiency and reduced pollution. With increased environmental concern for cleaner environment one must seek for ultra-low levels of pollutants emission (such as, NO_x, CO, unburned hydrocarbons and soot) from gas turbine powered energy and power conversion systems. The key factor to reduce emissions is uniform thermal flowfield (improved pattern factor) in the entire combustion zone that also helps to prevent local burnout of combustor with simultaneous benefits of increased turbine blade lifetime, higher firing temperatures and mitigation or elimination of cooling air requirements for both the combustor and turbine blades.

The colorless distributed combustion (CDC), which shares similar principles of the high temperature air combustion (HiTAC) [1],

* Corresponding author. Tel.: +1 301 405 5276; fax: +1 301 314 9477.
E-mail address: akgupta@umd.edu (A.K. Gupta).

http://dx.doi.org/10.1016/j.apenergy.2013.11.078
0306-2619/© 2014 Elsevier Ltd. All rights reserved.

has shown a novel option to achieve near zero emissions of NO_x and CO in addition to significantly improved pattern factor, stable combustion, alleviation of combustion instability, fuel flexibility, and low noise emission for high intensity gas turbine combustion application. The name colorless is due to negligible flame signatures as conventional flames in gas turbine combustors results in visible color besides the thermal signatures. Other attributes of colorless distributed combustion are given elsewhere [1–7].

Previous investigations on colorless distributed combustion (CDC) have demonstrated significant improvement in pattern factor, low noise emission levels and ultra-low emissions of NO_x and CO [2–7] and no requirements of a flame stabilizer under different flow configurations. The key requirement for colorless distributed combustion involves the avoidance of thin concentrated reaction zone and hot-spot zones in flames. This is achieved through controlled mixing between the combustion air and hot reactive gases so as to form hot and diluted oxidant stream followed by rapid mixing with the fuel stream. Alternatively fuel and/or air stream can also be mixed with the reactive gases. Such high temperature low oxygen concentration oxidant and its rapid mixing with the fuel foster distributed reaction condition so that even the lower reaction rate occupies larger volume with the same total fuel consumption. The reduced reaction rate was made possible through chemical reactions that occur at high reaction temperature, leading to relatively low temperature rise [1] in the combustion zone. In contrast, traditional normal oxygen concentration combustion results in sharp temperature rise with a very thin concentrated flame front with sharp temperature gradients. Such thin reaction zone results in hot spots that foster thermal NO_x emission produced from the Zeldovich thermal mechanism [8]. To form reactive oxidant stream, controlled entrainment of hot reactive gases is essential. The entrainment of hot reactive combustion gases into the fresh reactant stream can be achieved through proper design of the combustor flowfield.

Reactive gases entrainment into the fresh reactants for good preparation of the air–fuel mixture for ignition is of critical importance for low emission combustion. Entrainment can be obtained with different flow arrangements. One common practice used is to create recirculation and stabilize combustion with swirl flow that entrains and recirculates a portion of the hot combustion species back to the root of the flame. For such combustors swirl characteristics play a major role in mixing and combustion [9–11].

Another method to create recirculation zone involves the use of cyclone like configuration. Cyclone combustion chambers have been reported in many forms [9]. The key factors associated with such arrangement are longer residence time inside the combustor, large and multi-recirculation zones and high turbulence levels generated from the high shear between differing fluid, as well as large toroidal recirculation zone. High turbulence levels are generated for center exit configuration. Other beneficial aspects of such flow configuration and detailed description of their application are given [9].

In almost all these arrangements, the recirculation of hot product gases is achieved through two key features. The first is the air jet entrainment, wherein the inlet air jet entrains flow from the surrounding gases present. The second is the internally recirculated gases due to the role of swirl. Numerous studies have been reported on the jet entrainment. Ricou and Spalding [12] provided a simple relationship for the entrainment which can be modified to give entrained mass flux as follows:

$$\mathrm{mdot_{ent}}/\mathrm{mdot_o} = 0.32 * (x/d^*) - 1 \quad (1)$$

where d^* is given by: $d^* = d_o\,(\rho_o/\rho_\infty)^{1/2}$ and $\mathrm{mdot_{ent}}$ is the entrained mass flux, $\mathrm{mdot_o}$ is the initial jet mass flux and x is the downstream distance, d_o is the jet diameter, ρ_o is the initial jet density and ρ_∞ is the surrounding density [12]. Han and Mungal [13] quantified the effect of different parameters on jet entrainment, such as, heat (energy) release and buoyancy relating to reacting cases with view to predict NO_x emission in a lifted jet flame. However, when the air jet is enclosed in the combustor, the entrainment rate is expected to be different as the surrounding media cannot be considered as a free stream anymore. Also, this expression only considers jet entrainment without considering any recirculated mass flow rate due to the combustor geometry.

Cylindrical colorless distributed combustion incorporating tangential air injection has been investigated with emphasis on ultra-low pollutants emission and distributed reaction to explore the environmental advantages of such flows [4–6]. Similar configurations have been examined with different aspect ratio [14–16]. However, these investigations were for furnace applications, which are characterized by low heat (energy) release intensity (0.1–1 MW/m^3 atm.) as compared to high heat (energy) release (20–50 MW/m^3 atm.) distributed combustion [4–6] for gas turbine applications. It is to be noted that all practical gas turbine combustors operate at high pressures so that the data obtained at normal and elevated pressures can be correlated if expressed in terms of MW/m^3 atm [17]. For the swirling colorless distributed combustion [4–6], air is injected tangentially into the combustion chamber at high air velocity to form swirling motion. This air jet entrains large amounts of hot reactive combustion gases forming a recirculation zone. The amount of recirculation is controlled so that it increases the temperature of the air and reactive gases above the auto-ignition temperature of the fuel. The uniformly mixed fuel/air/reactive gases then spontaneously ignite to result in a distributed reaction regime, instead of a thin concentrated reaction flame front in normal flames. Hence, it may be noted that CDC cases discussed differ from conventional gas turbine flames in that it does not require a flow reversal or low velocity region for flame stabilization. The hot reactive gases mix with the fresh mixture and increase the temperature of the mixture to high enough temperatures for spontaneous ignition of the mixture in the entire combustion zone as compared to only small region of the fresh mixture for flame stabilization in conventional flames.

The effect of hot recirculated combustion gases on the flame characteristics have been studied [18]. The recirculated gases ratio to fresh air stream was varied between 0% and 950%, leading to oxygen concentration variation in the hot diluted oxidizer between 21% and 2%, respectively. It was shown that the flame size and volume increased with increase in fresh stream temperature and decrease in oxygen concentration. The high temperature air combustion occurred under certain conditions of controlled mixing between recirculated hot reactive species and low oxygen concentration air. Note that high temperature air combustion is different than flameless combustion wherein the oxygen concentration is very low with much of the heat exchange occurs from mass transfer between the fluids. Also OH, CH, and C_2 radicals, captured through chemiluminescence, occupied larger portion of the combustion chamber at low oxygen concentration compared to high oxygen concentration. The emission of NO_x was significantly reduced from about 1500 ppm (0% recirculation) down to 300 ppm, 20 ppm, and 10 ppm for recirculation ratios of 40%, 320%, and 950%, respectively at hot oxidizer temperature of 1273 K [18].

The non-reacting flowfield of swirling and non-swirling configurations have been previously characterized with focus on recirculation generation for achieving colorless distributed combustion and enhance thermal and environmental performance of the combustor with ultra-low emissions. Non-reacting flowfield helps to understand the flow characteristics inside the combustor along with the turbulence generated and the mixing characteristics. It was concluded that swirling CDC generates higher entrainment inside the combustor compared to the non-swirling configuration

[19] which is in agreement with ultra low pollutants emission obtained from swirling configuration as compared to non-swirling one [4].

Different researchers have investigated the effect of reactants injection velocity on pollutants emission. Kim et al. [20] investigated the effect of fuel air mixing on NO_x emission in non-premixed flames with coaxial air using hydrogen and diluted hydrogen as fuels. The major parameters used to modify mixing were the fuel jet velocity and coaxial air velocity. Chen and Driscoll [21] investigated the effect of coaxial air amount on the behavior of jet diffusion flame. They concluded that for hydrogen flames, six folds reduction in NO_x emission index was achieved with increased coaxial air velocity to fuel velocity. However, such reduction was not demonstrated with methane flame as the emission index of NO_x (EINOX) slightly increased with increase in the co-axial air to fuel velocity [21]. Other researchers investigated the effect of jet momentum and injection velocities on the formation of flameless combustion and associated NO_x emission [22]. It was concluded that increasing injection velocity decreases NO_x emission at a constant equivalence ratio of 0.77. However, flameless oxidation could not be established for equivalence ratios lower than 0.59 which is more relevant to gas turbine applications [22].

In this paper, the effect of air injection velocity on combustor flowfield with special focus on pollutants emission is investigated. The isothermal flowfield for different air inlet velocities are characterized, with emphasis on entrainment (recirculation) and turbulence generation. Pollutants emission from reacting flow experiments are presented at different air injection velocities with view to develop relationship between injection velocity and combustor performance under both premixed and non-premixed combustion modes under high intensity combustion condition.

2. Experimental

The combustor performance was examined using different air injection velocities at a nominal heat load of 6.25 kW and heat (energy) release intensity of 36 MW/m^3 atm. The combustion chamber was cylindrical with air injected tangentially at half the height of chamber for all the cases reported here. Fuel was also injected at the same plane as air injection. For enhancing the residence time of reactants in the combustor, a tube was extended inside the combustor for product gases exiting the combustor. Fig. 1 shows a schematic diagram of the combustor used. More detailed description of the combustor geometry is given elsewhere [5].

The combustor was modified at the air injection plane to allow optical access for flowfield examination using particle image velocimetry as the diagnostics, see Fig. 1. The camera located at a distance of 0.3 m away from the laser plane covered a test region of 4.4 cm × 3.36 cm. The camera was mounted on a traverse mechanism to allow full flowfield examination inside the combustor. Further details on the PIV setup, the seeding particles, and seeding mechanism are given elsewhere [19,23].

The seed air, representing 5% of the total combustion air flow supplied, was mixed with the seed particles for introducing the particles into the combustor. Approximately 1 mm thick laser sheet beam was used to illuminate the seed particles in the flow. For interrogation window size, adaptive mode was used wherein the correlation is calculated on a subset of the grid points using an interrogation size of at least 24 pixels. The results were validated and used as 'predicted' vector values. Then the correlation was calculated and the predicted values used as a local offset for the delayed image.

For reacting flow both air and gaseous fuel flow rates were measured using choked flow orifice systems. Precision stainless steel orifices were used to choke the flow of the gases and upstream pressure was controlled to supply the required mass flow rate of gases. The upstream pressure was controlled using pressure regulators to maintain a steady pressure and avoid any oscillations in pressure due to compressor turning on and off periodically. The upstream pressure for both air and fuel was maintained between ±0.2 psi of the desired pressure. The pressure was measured using a piezoresistive digital pressure gauge with accuracy of ±0.25psi. It was ensured that the downstream pressure was lower than the pressure required for choking the flow based on the upstream pressure.

Detailed investigations on the overall emissions from the combustor as well as visible emissions have been performed for the various experimental conditions. The concentration of NO was measured using a NO–NO_x chemiluminescent gas analyzer; CO concentration was measured using the non-dispersive infrared method and O_2 concentration (used to correct the NO and CO emissions at standard 15% oxygen concentration) was measured using galvanic cell method. During a single experiment, measurements were repeated at least three times for each configuration and the uncertainty was estimated to be about ±0.5 ppm for NO and ±10% for CO emission. A photograph of the experimental test rig is shown in Fig. 2.

The investigations performed on experimental combustor were aimed at comparing the performance of combustor with different air injection velocities. The facility allowed variation of the injection velocity and nozzle diameter of the fuel and air as well as hot gasses exit. Table 1 summarizes the cases reported here. For each case the fuel flow rate was changed to achieve different equivalence ratios. The respective case name indicates the premixed and non-premixed combustor geometry (ATP, ATF) and the air injection diameter.

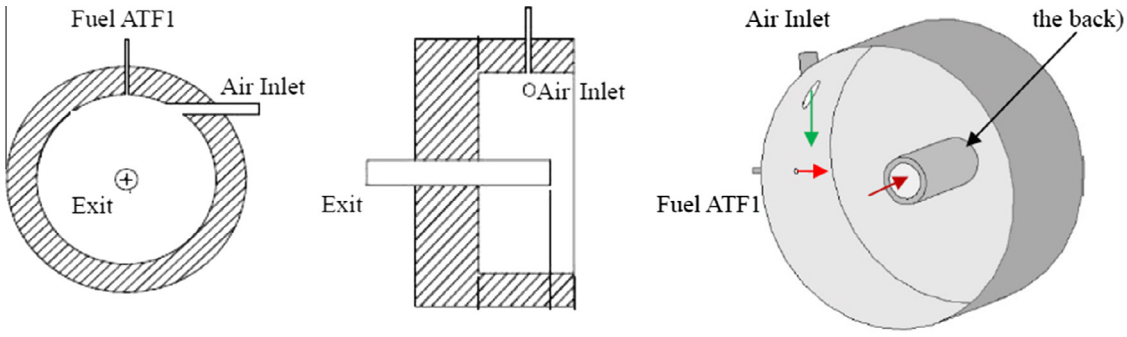

Fig. 1. A schematic diagram of the combustor with extended axial exit "ATP and ATF-1" (left: top section at mid location, middle: front section at cylinder axis, and right: 3-D geometry).

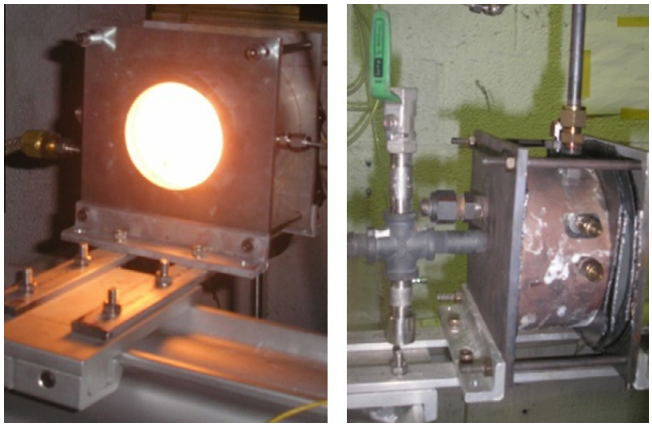

Fig. 2. High intensity CDC cylindrical combustor test rig showing (left) optical access and (right) axial product gas exit.

Table 1
Experimental test matrix.

Case No.	Injection velocity (m/s)	Air injection temperature (K)	Mode
ATP-31	46	300	Premixed
ATP-24	78	300	Premixed
ATP-20	103	300	Premixed
ATP-T-31	92	600	Premixed
ATP-T-24	156	600	Premixed
ATP-T-20	206	600	Premixed
ATF1-T-31	92	600	Non-premixed
ATF1-T-24	156	600	Non-premixed
ATF1-T-20	206	600	Non-premixed

3. Flowfield and turbulence

Particle image velocimetry was used to determine the flow velocity and turbulence characteristics under non-reacting conditions. The velocity data presented here is on U and V mean velocity and velocity vectors, where U and V are the velocity components in the X and Y directions respectively. Note that the extended hot product gases exit tube inside the combustor resulted in an "optical blind spot", wherein no light was present to illuminate the particles due to obstruction of the laser sheet beam. Results from the two injector diameters are reported (ATP-31and ATP-24) at flow injection velocities of 46 and 78 m/s. Fig. 3 shows the obtained velocity vectors and velocity magnitudes for the ATP-31 configuration. Fig. 4 shows the corresponding data for ATP-24 configuration.

Flowfield data on men velocity and velocity vectors showed that both configurations results in similar mean flow behavior; however, the velocity magnitudes were higher in the configuration ATP-24 due to the higher air injection velocity at the inlet. The higher injection velocity resulted in a higher recirculated mass flow rates. The recirculation ratio for this configuration was calculated for the investigated plane (shown in Figs. 3 and 4), and is defined as:

$$R_{\text{circulation}} = (\text{mdot}_{\text{tot}} - \text{mdot}_{\text{air}})/\text{mdot}_{\text{air}} \tag{2}$$

where mdot_{tot} is the total flow rate crossing a plane, and mdot_{air} is the inlet mass flow rate. Rearranging in terms of velocity and adopting a line for calculation in a 2-D plane, we get

$$R_{\text{circulation}} = (V_{\text{line}} * L_{\text{line}} * t_{\text{line}} - V_{\text{air}} * d_{\text{air}} * t_{\text{line}})/(V_{\text{air}} * d_{\text{air}} * t_{\text{line}}) \tag{3}$$

where V_{line} is the average velocity perpendicular to the examined line, L_{line} is the length of the examined line, V_{air} is the air jet inlet axial velocity, d_{jet} is the air jet diameter and t_{line} is thickness of the examined line where the 2-D plane is $t_{\text{line}} * L_{\text{line}}$.

Following Eq. (3), it was found that the recirculation ratio increased by some 15% with higher air injection velocity (i.e., for case ATP-24 as compared to case ATP-31).

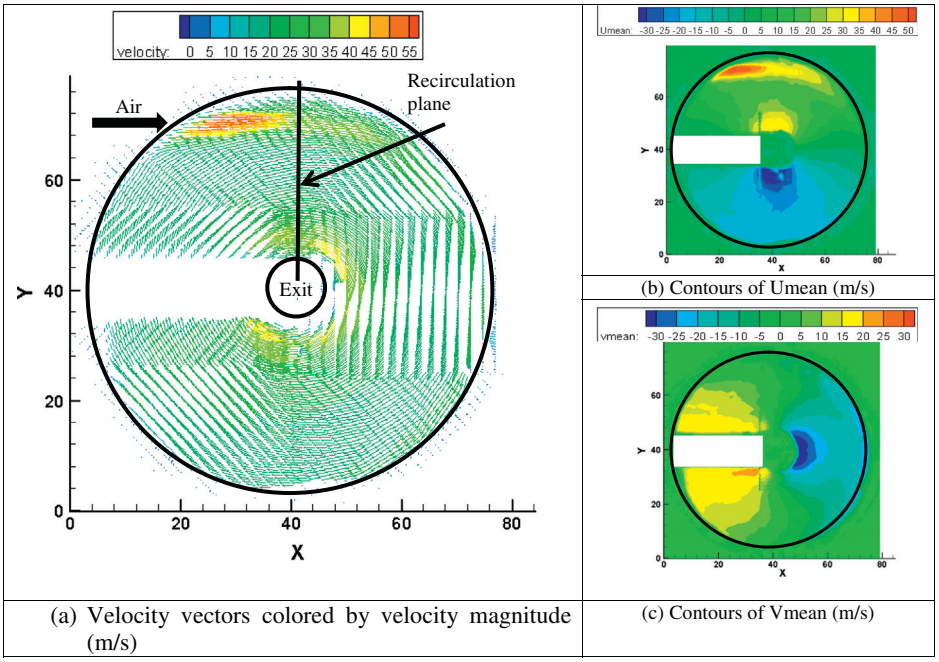

(a) Velocity vectors colored by velocity magnitude (m/s)

(b) Contours of Umean (m/s)

(c) Contours of Vmean (m/s)

Fig. 3. (a) Velocity vectors, (b) U mean, and (c) V mean for configuration ATP-31.

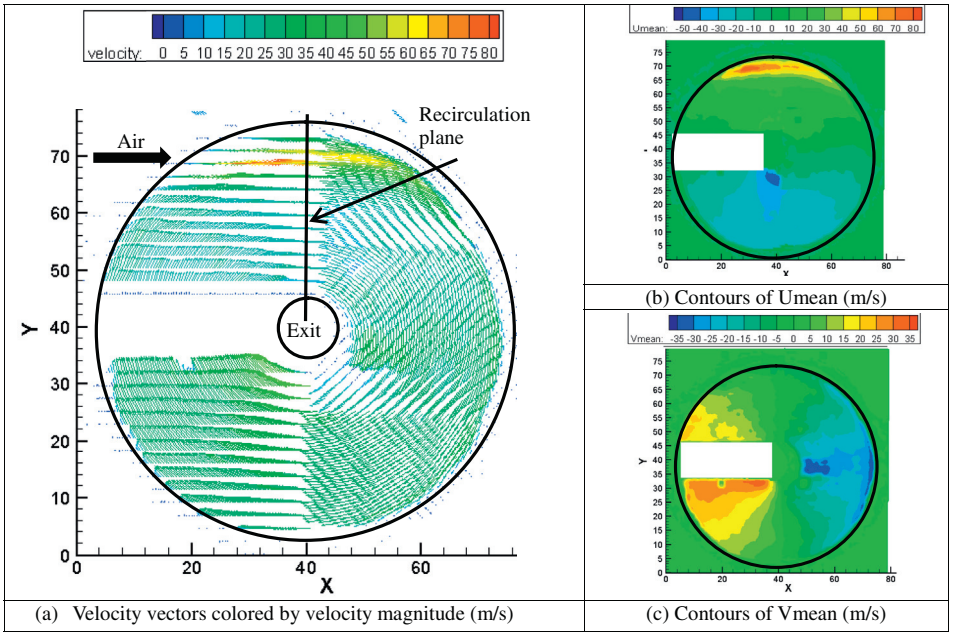

(a) Velocity vectors colored by velocity magnitude (m/s)

(b) Contours of Umean (m/s)

(c) Contours of Vmean (m/s)

Fig. 4. (a) Velocity vectors, (b) *U* mean, and (c) *V* mean for configuration ATP-24.

The velocity fluctuation at the inlet region was also found to increase with increase in the air injection velocity. Fig. 5 shows the velocity fluctuations (U_{rms}) along the *X*-direction for the region covering the entry jet. It can be seen that for configuration ATP-31, the velocity fluctuation had a maximum intensity of 17 m/s at the entry jet. On the other hand, for configuration ATP-24, the velocity fluctuation had a maximum of 40 m/s, more than double that of configuration ATP-31, though the inlet velocity increased by only 70%.

The increased turbulence at inlet is expected to play an important role in the mixture preparation process between fresh mixtures and hot active gases from within the combustor to promote distributed combustion condition. For non-premixed cases, increased turbulence will play a critical role as the mixing of the fuel jet in cross flow direction is mainly dominated by turbulence in both near and far field for the low velocity ratios [24]. The overall high flow velocity is expected to prevent flame anchoring, eliminating local hot spots, which is important for ultra-low emissions.

4. Results and discussion on pollutants emission

4.1. Premixed case using normal temperature air

Experimental results on pollutants emissions for cases ATP-31, ATP-24 and ATP-20 are now presented. These cases were investigated with air injection at room temperature as shown in Table 1. Fig. 6 shows NO emission for the different cases, wherein the effect of injection velocity on NO emissions can be seen. Increasing the injection velocity from 46 m/s (ATP-31) to 78 m/s (ATP-24) decreased NO emissions by about 13% for the different equivalence ratios presented here. Further increase in air injection velocity up to 103 m/s (ATP-20) resulted in decreased NO emission by 20% compared to the injection velocity for the case of ATP-31. Such a decrease in NO emission can be related to the enhanced entrainment of hot recirculated gases (as indicated by isothermal flow filed) with higher air injection velocities, which promotes distributed reaction condition.

Fig. 7 shows the experimentally measured CO emissions for different air injection velocities discussed earlier. It can be seen that the velocity affected CO emissions to some extent as emission increased with increase in air injection velocity. This is attributed to the decrease in residence time inside the combustor with increase in the injection velocity.

4.2. Premixed case using 600 K preheated air

The experimental data with inlet air preheated to 600 K temperature, simulating the combustor intake temperature after the compressor, are now presented. With preheated air, NO emission increased while CO emission decreased [5]. Note that the increase in air inlet temperature from 300 K to 600 K doubled the air injection velocity as shown in Table 1. Fig. 8 shows the NO emissions for the three cases of ATP-T-31, ATP-T-24 and ATP-T-20. Increasing injection air velocity decreased the NO emissions by some 25%

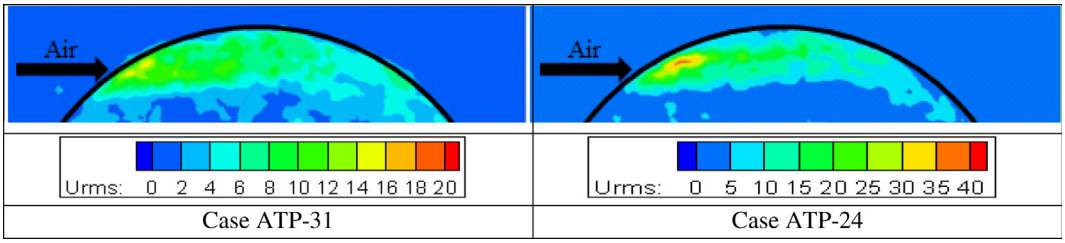

Case ATP-31 Case ATP-24

Fig. 5. Velocity fluctuations (U_{rms}) at the jet entry region.

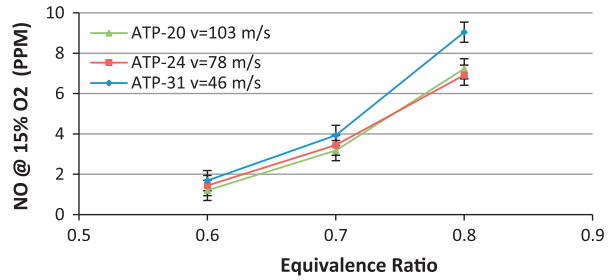

Fig. 6. NO emissions for different injection velocities, inlet air temperature = 300 K.

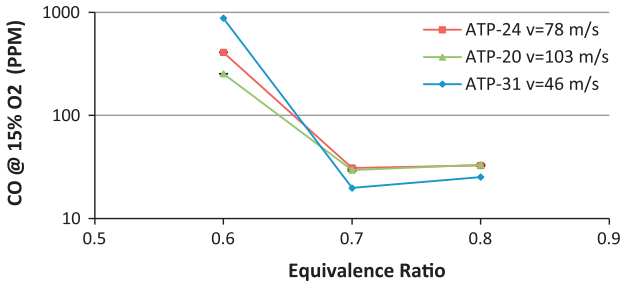

Fig. 7. CO emissions for different injection velocities, inlet air temperature = 300 K.

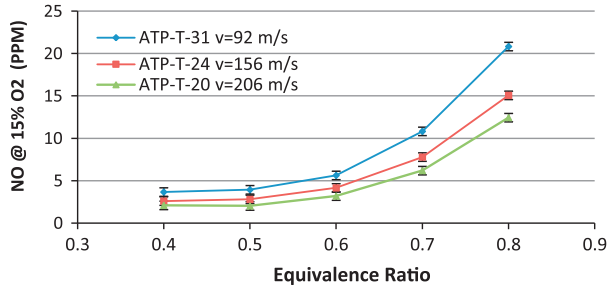

Fig. 8. NO emissions for different injection velocities, inlet air temperature = 600 K.

(compare cases ATP-T-31 and ATP-T-24) and by 45% (compare the cases ATP-T-31 and ATP-T-20). At an equivalence ratio of 0.6, NO emissions were decreased from 5.6 ppm (case ATP-T-31) to 4.15 ppm (case ATP-T-24) and then to 3.19 ppm (case ATP-T-20). Such reduction emphasizes the important role of air injection velocity and its effect on emissions through prevention of flame anchoring and enhanced mixing. Lower emissions were also obtained at lower equivalence ratios with only 2 ppm at an equivalence ratio of 0.5 (for case ATP-T-20).

Fig. 9 shows experimentally measured CO emission for different air injection velocities with air preheated to 600 K. The trend obtained with these measurements agrees with the previous case data at 300 K wherein the increase in air injection velocity increased the CO emissions. This is attributed to decreased residence time inside the combustor with increase in injection velocity. However, the increase in CO emissions with increase of air injection velocity was less compared to the 300 K temperature air injection. This is directly attributed to the effect of air preheats on CO emission. The CO emissions decreased with increase in inlet air temperature under lean combustion conditions [5]. The increase in temperature aids in complete conversion of CO to CO_2 and shifts the minimum CO points to even more lean condition as compared to the non-preheated air case.

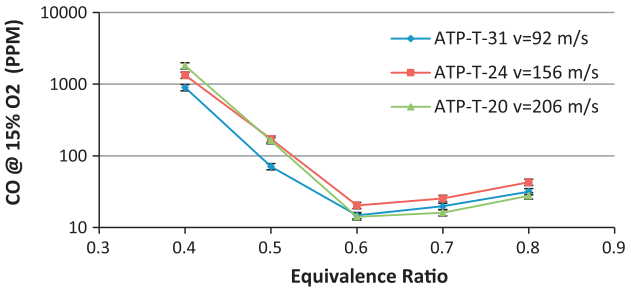

Fig. 9. CO emissions for different injection velocities, inlet air temperature = 600 K.

The radical intensity distribution of OH^* chemiluminescence for cases ATP-T-31 and ATP-T-20 are shown in Fig. 10. For the different equivalence ratios examined, the results show that the reaction starts farther downstream for case ATP-T-20 as compared to ATP-T-31. This can be attributed to higher air injection velocity that leads to the onset of flame further downstream. As the flame reaction zone moves farther downstream, more time is given prior to spontaneous ignition. This allows for better mixing between the injected mixture of air and fuel and the recirculated hot reactive species. Also it can be seen that the reaction is more distributed in the case ATP-T-20 as compared to ATP-T-31, especially at higher equivalence ratios of 0.8 and 0.7, wherein higher OH^* signal was recorded away from the main reaction zone. Relating reaction behavior (obtained through OH^* chemiluminescence) and pollutants emission, one can see the desirable impact of higher injection velocities on NO emission. The NO emission levels decreased from 21 ppm to 12.5 ppm at an equivalence ratio of 0.8 (wherein the reaction zone is more distributed). This reduction in emissions is directly attributed to better mixture preparation prior to ignition and the resulting enhanced reaction zone distribution. For all the cases, the reaction intensity decreased and moved further downstream with decrease in equivalence ratio, see Fig. 10.

4.3. Non-premixed case with preheated air

Non-premixed examination with inlet air preheated to 600 K, simulating the combustor intake temperature after the compressor, yielded similar results. Fig. 11 shows the recorded NO emissions for the three cases of ATF1-T-31, ATF1-T-24 and ATF1-T-20. Increase in injection air velocity decreased NO emission by 24% (compare cases ATF1-T-31 and ATF1-T-24) and by 46% (compare cases ATF1-T-31 and ATF1-T-20). At an equivalence ratio of 0.6, NO emissions decreased from 9.6 ppm (case ATF1-T-31) to 7.33 ppm (case ATF1-T-24) and to 5.82 ppm (case ATF1-T-20). Such reduction emphasizes the important role of air injection velocity on emissions through prevention of flame anchoring and enhanced mixing in both premixed and non-premixed combustion mode. Under non-premixed combustion, ultra-low emission of NO was demonstrated at an equivalence ratio of 0.5 (2.28 ppm of NO) for case ATF1-T-20.

This reduction might be somewhat unexpected. As the air injection velocity increases, the velocity ratio between the cross flow and the fuel jet dramatically decreases from 1.108 (case ATF1-T-31) to 0.495 (case ATF1-T-20). The velocity ratio is defined as [24]:

$$VR = \left[\left(\rho_j v_j^2\right)/\left(\rho_{cf} v_{cf}^2\right)\right]^{1/2} \quad (4)$$

where ρ is the density, v is the velocity, and the subscripts j stands for the fuel jet, cf stands for crossflow [24]. As the velocity ratio decreases, the fuel jet penetration decreases [25]. This affects mixing dramatically; however, this effect is reversed by the dominance

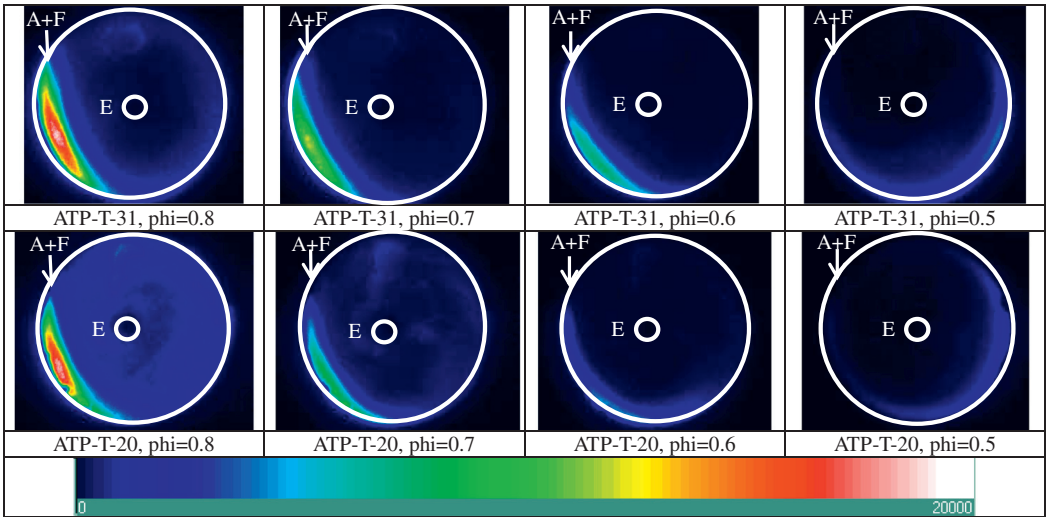

Fig. 10. OH^* chemiluminescence for cases ATP-T-31 and ATP-T-20.

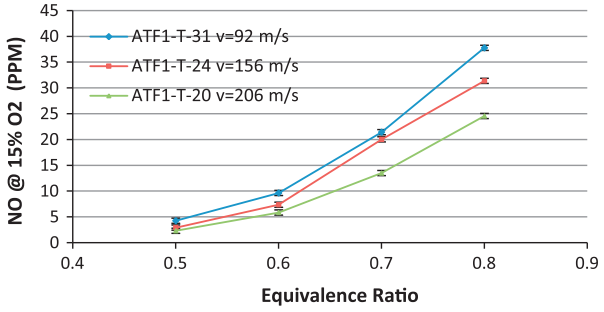

Fig. 11. NO emissions for different injection velocities. Non-premixed, inlet air temperature = 600 K.

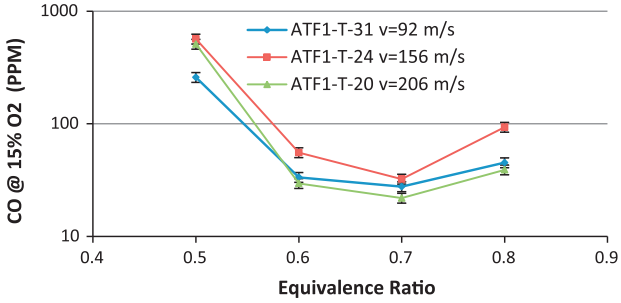

Fig. 12. CO emissions for different injection velocities. Non-premixed, inlet air temperature = 600 K.

of turbulence at such low velocity ratios. The turbulence is enhanced through increase in the air injection velocity (increasing the cross flow velocity) as shown in Fig. 5 leading to an overall enhanced mixing and lower NO emissions.

Fig. 12 shows the experimentally measured CO emissions for different air injection velocities with air preheated to 600 K under non-premixed combustion condition. The trend obtained with these measurements agrees with the previously measured data wherein the increase in air injection velocity increased CO emission. This is specifically true comparing the cases ATF1-T-31 and ATF1-T-24. For case ATF1-20, CO emissions were actually lower compared to the other cases (ATF1-T-31 and ATF1-T-24).

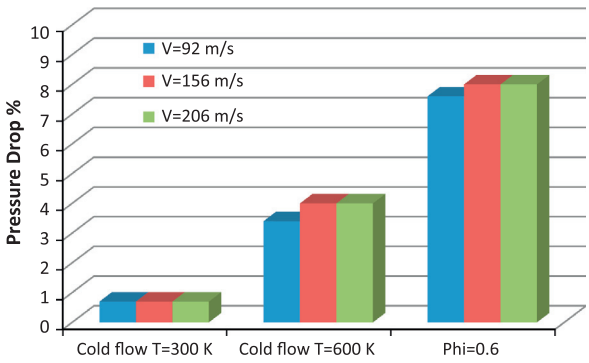

Fig. 13. Percent pressure loss for different air injection velocities.

4.4. Pressure loss

Lower pressure loss is desirable to achieve higher efficiency from the gas turbines. Previous researches have indicated that the higher the air injection velocity, the bigger the pressure drop will be in the combustor [26]. Pressure loss across for the CDC combustor with air preheated to 600 K was measured and is presented in Fig. 13. The results show that pressure loss is less than 8% at the most desirable operating condition (at an equivalence ratio of 0.6). Pressure loss is observed to increase with equivalence ratio possibly due to higher heat addition at higher equivalence ratios. Pressure loss measured with inlet air at temperature of 600 K and 300 K is also shown in Fig. 13.

5. Distributed combustion

The development of an "Index" that characterizes the extent of distributed reaction within the combustor in terms of different geometrical and operational parameters are important for seeking such distributed reaction. One can envision an index which relates the actual combustion parameters for the extent of distributed combustion conditions. Such a distributed index (DI) may include, amongst other parameters, recirculation ratio (entrainment rate), injection velocity for enhanced mixing, injection configuration (premixed and non-premixed) with distance between different

injectors, and the fresh reactants conditions (temperature and pressure) [19], i.e.,

$$\mathrm{DI} = f(ent) * f(velocity) * f(configuration) * f(temp\ \&\ pressure) \quad (5)$$

From the pollutants emissions, OH* chemiluminescence, and velocity data, one can deduce that air injection velocity plays an important role for distributed reaction. Isothermal PIV data on the flow velocity have shown that increase in velocity increases the recirculation ratio and enhances mixing through turbulence, while OH* chemiluminescence showed that the reaction started further downstream at higher velocities as compared to lower velocities. For the recirculation enhancement, a simple relation was proposed, wherein the percentage of product gases and reactive species in the ignition mixture is normalized by the value required for optimum performance (85.7%), resulting in an optimum distributed reaction condition value of 1 [19].

Using the PIV data on flowfield at two examined velocities, it was found that for injection velocity of 46 m/s, the recirculation ratio was 1.25, which increased to 1.4375 with and injection velocity of 78 m/s. Thus, a percentage of reactive gases of 55.5% and 58.9% were achieved, leading to a $f(ent)$ value of 0.65 and 0.69, respectively. Now using these two values, a linear fit can be obtained, wherein the recirculation ratio can be plotted as a function of injection velocity as:

$$\text{Recirculation Ratio} = 0.0059 \times \text{Air injection velocity} + 0.9805 \quad (6)$$

Using the approximation, a recirculation ratio for air injection velocity of 103 m/s can be calculated and was found to be 1.59 leading to a reactive gas percentage of 61.3% and $f(ent)$ value of 0.72.

Now for the velocity portion of the DI, $f(velocity)$, it is desired to quantify the relationship between injection velocity and mixing time scale along with pollutants emission. Mixing time scale can be defined on integral scale as:

$$\tau_{\mathrm{flow}} = (l_o / v_{\mathrm{rms}}) \quad (7)$$

where l_o is the integral length scale (approximated to $d_{\mathrm{jet}}/10$, where d_{jet} is the jet diameter, while v_{rms} is the turbulent velocity. Following this definition, the mixing time scale for the injection velocities of 46 m/s and 78 m/s were 0.0794 ms and 0.022 ms, respectively. These mixing time scales are small compared to the typical residence time in a gas turbine combustor of 2–10 ms, and are below the values implemented by some researchers (about 0.08 ms) [27]. On the other hand, if we relate NO emissions with injection velocities, the impact of injection velocity on NO emission is evident as seen in Fig. 14.

From this plot, it can be seen that NO approaches a minimum value as the velocity increases. Such minimum value is envisioned to be dictated by NO formation routes other than the Zeldovich (thermal) mechanism, such as, prompt (Fenimore) mechanism. Consequently, the optimum injection velocity may be assumed to be around 100 m/s. The same plot is obtained for experiments where preheated air was employed. The data suggests that as the velocity approaches 200 m/s, a minimum of NO emissions is approached for this operational condition (see Fig. 15).

Using the above data, an expression is developed to show the impact of the injection velocity on distributed reaction. Optimum injection velocity is envisioned to be 100 m/s for normal air temperature and 200 m/s for 600 K air injection temperature. Thus, an expression relating the actual velocity used to the optimum velocity can be formulated as:

$$f(velocity) = v_{\mathrm{injection@300K}}/100 \quad (8)$$

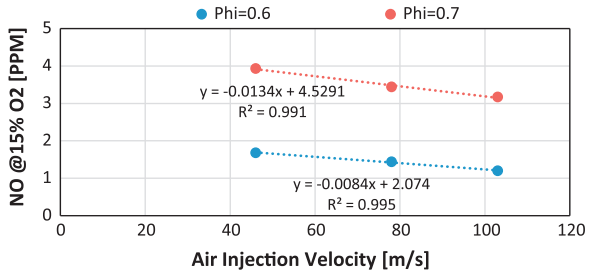

Fig. 14. Effect of air injection velocity on NO emissions.

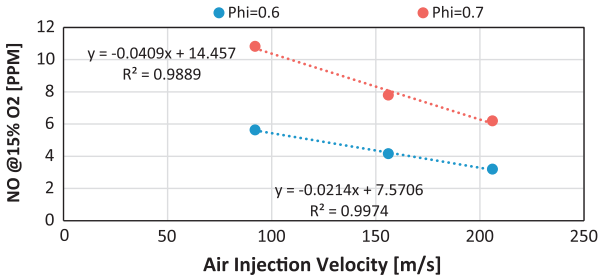

Fig. 15. Impact of air injection velocity on NO emissions for air inlet temperature of 600 K.

where $v_{\mathrm{injection@300K}}$ is the air injection velocity at 300 K. For injection at other temperatures, the velocity can be corrected through the following expression:

$$v_{\mathrm{injection@300K}} = v_{\mathrm{injection@T}} \times (\rho_{@T}/\rho_{@300K}) \quad (9)$$

The expression for distribution index becomes:

$$\mathrm{DI} = (\text{Reactive gas }\%/85.7\%) \times (v_{\mathrm{injection@300K}}/100) \times f(configuration) \times f(temp\ \&\ pressure) \quad (10)$$

where the reactive gas % can be calculated through the recirculation ratio using the form,

$$\text{Reactive gas }\% = \text{Recirculation Ratio}/(\text{Recirculation Ratio} + 1) \quad (11)$$

Further studies will be performed to obtain similar relationships for the air and fuel injection configuration as well as temperature and pressure effects to fully identify the distribution index.

6. Conclusions

Experimental investigations provided here outline the important role of air injection velocity and recirculation on the reduction of pollutants emission. Flowfield data using particle image velocimetry showed increased recirculation ratio and turbulence (velocity fluctuations) in the combustor with increase in air injection velocity. Increased recirculation ratio is critical for the mixing of hot reactive species with fresh air and fuel stream. Increased turbulence aids in mixing between these streams to result in an improved distributed combustion reaction to occur as compared to lower air injection velocity.

Pollutants emission measured for different air injection velocities showed that higher air injection velocity results in lower NO emission. Increase in injection velocity from 46 m/s to 103 m/s reduced NO emission by about 20%. With air preheats under premixed condition, the NO emission at an equivalence ratio of 0.6 was 5.6 ppm at air injection velocity of 92 m/s. Increasing the air injection velocity to 206 m/s reduced this NO to 3.2 ppm

(44% reduction). NO Emission as low as 2 ppm was obtained at increased air injection velocity. The increase in air injection velocity did not impart large pressure drop in the combustor as the pressure drop for reacting cases remained almost constant for the different velocities examined.

The impact of air injection velocity on pollutants emissions is provided with view to develop a distribution index (DI) that describes the extent of uniform distributed reactions within the combustor. Such distribution index depends, amongst other parameters, on entrainment (recirculation) of reactive species, injection velocity, air and fuel injection configuration, and operational temperature and pressure. The role of air injection velocity on the DI is provided, where the air injection velocity was normalized by the optimal injection velocity to achieve distributed conditions. Additional future studies will help provide similar relations for the remaining parameters for full development of the distributed index.

Acknowledgments

This research was supported by ONR, Program Managers, Dr. Gabriel D. Roy and Dr. Clifford Bedford, and DLA. This support is gratefully acknowledged.

References

[1] Tsuji H, Gupta AK, Hasegawa T, Katsuki M, Kishimoto K, Morita M. High temperature air combustion: from energy conservation to pollution reduction. CRC Press; 2003.
[2] Arghode VK, Gupta AK. Effect of flow field for colorless distributed combustion (CDC) for gas turbine combustion. J Appl Energy 2010;78:1631–40.
[3] Arghode VK, Gupta AK. Investigation of forward flow distributed combustion for gas turbine application. J Appl Energy 2010;88:29–40.
[4] Khalil AEE, Gupta AK. Swirling distributed combustion for clean energy conversion in gas turbine applications. J Appl Energy 2011;88:3685–93.
[5] Khalil AEE, Gupta AK. Distributed swirl combustion for gas turbine application. J Appl Energy 2011;88:4898–907.
[6] Khalil AEE, Gupta AK, Bryden MK, Lee SC. Mixture preparation effects on distributed combustion for gas turbine applications. J Energy Resour Technol 2012;134(3):032201.
[7] Arghode VK, Khalil AEE, Gupta AK. Fuel dilution and liquid fuel operational effects on ultra-high thermal intensity distributed combustor. J Appl Energy 2012;95C:132–8.
[8] Correa SM. A review of NO_x formation under gas-turbine combustion conditions. Combust Sci Technol 1992;87:329–62.
[9] Gupta AK, Lilley DG, Syred N. Swirl flows. Tunbridge Wells, England: Abacus Press; 1984.
[10] Archer S, Gupta AK. Effect of swirl on flow dynamics in unconfined and confined gaseous fuel flames. In: 42nd AIAA Aerospace Sciences Meeting and Exhibit 5–8 January 2004, Reno, Nevada; 2004.
[11] Leuckel IW, Fricker N. The characteristics of swirl-stabilized natural gas flames. J Inst Fuel 1976;49:103–12.
[12] Ricou FP, Spalding DB. Measurements of entrainment by axisymmetrical turbulent jets. J Fluid Mech 1961;11(1):21–32.
[13] Han D, Mungal MG. Direct measurement of entrainment in reacting/nonreacting turbulent jets. Combust Flame 2001;124:370–86.
[14] Baluev ED, Troyankin YV. The effect of the design parameters on the aerodynamics of cyclone chambers. Thermal Eng 1967;14(2):67–71.
[15] Ustimenko BP, Bukhman MA. Turbulent flow structure in a cyclone chamber. Thermal Eng 1968;15(2):64–7.
[16] Yetter RA, Glassman I, Gabler HC. Asymmetric Whirl combustion: a new low NO_x approach. Proc Combust Inst 2000;28:1265–72.
[17] Vincent ET. The theory and design of gas turbines and jet engines. 1st ed. McGraw-Hill Book Co.; 1950.
[18] Gupta AK, Bolz S, Hasegawa T. Effect of air preheat temperature and oxygen concentration on flame structure and emission. J Energy Resour Technol 1999;121(3):209–17.
[19] Khalil AEE, Gupta AK. Swirling flowfield for colorless distributed combustion. J Appl Energy 2014;113:208–18.
[20] Kim S, Yoon Y, Jeung I. Nitrogen oxides emissions in turbulent hydrogen jet nonpremixed flames: effects of coaxial air and flame radiation. Proc Combust Inst 2000;28:463–71.
[21] Chen R, Driscoll F. Nitric oxide levels of jet diffusion flames: effects of coaxial air and other mixing parameters. In: 23rd symposium (international) on combustion, vol. 23. The Combustion Institute; 1990. p. 281–8.
[22] Verissimo AS, Rocha AMA, Costa M. Importance of the inlet air velocity on the establishment of flameless combustion in a laboratory combustor. Exp Therm Fluid Sci 2013;44:75–81.
[23] Arghode VK, Gupta AK, Bryden KM. High intensity colorless distributed combustion for ultra low emissions and enhanced performance. J Appl Energy 2012;92:822–30.
[24] Smith SH, Mungal MG. Mixing, structure and scaling of the jet in crossflow. J Fluid Mech 1998;357:83–122.
[25] Andreopoulos J, Rodi I. Experimental investigation of jets in a crossflow. J Fluid Mech 1984;138:93–127.
[26] Bobba MK. Flame stabilization and mixing characteristics in a stagnation point reverse flow combustor. PhD Dissertation-Georgia Institute of Technology, 2007.
[27] Arghode VK. Development of colorless distributed combustion for gas turbine application. PhD Dissertation-University of Maryland, 2011.